

## Analysis of composite girders with hybrid GFRP hat-shape sections and concrete slab

Elham Alizadeh<sup>a</sup> and Mehdi Dehestani\*

*Faculty of Civil Engineering, Babol Noshirvani University of Technology, Babol, Iran*

*(Received October 24, 2014, Revised March 29, 2015, Accepted April 4, 2015)*

**Abstract.** Most of current bridge decks are made of reinforced concrete and often deteriorate at a relatively rapid rate in operational environments. The quick deterioration of the deck often impacts other critical components of the bridge. Another disadvantage of the concrete deck is its high weight in long-span bridges. Therefore, it is essential to examine new materials and innovative designs using hybrid system consisting conventional materials such as concrete and steel with FRP plates which is also known as composite deck. Since these decks are relatively new, so it would be useful to evaluate their performances in more details. The present study is dedicated to Hat-Shape composite girder with concrete slab. The structural performance of girder was evaluated with nonlinear finite element method by using ABAQUS and numerical results have been compared with experimental results of other researches. After ensuring the validity of numerical modeling of composite deck, parametric studies have been conducted; such as investigating the effects of constituent properties by changing the compressive strength of concrete slab and Elasticity modulus of GFRP materials. The efficacy of the GFRP box girders has been studied by changing GFRP material to steel and aluminum. In addition, the effect of Cross-Sectional Configuration has been evaluated. It was found that the behavior of this type of composite girders can be studied with numerical methods without carrying out costly experiments. The material properties can be modified to improve ultimate load capacity of the composite girder. strength-to-weight ratio of the girder increased by changing the GFRP material to aluminum and ultimate load capacity enhanced by deformation of composite girder cross-section.

**Keywords:** composite girders; GFRP; hat-shape section; nonlinear finite element analysis; ABAQUS

### 1. Introduction

Bridge deck is a structural member that dispenses loads transversely to the girders that bear on piers or abutments. The bridge deck performs a vital role in a bridge system and its durability affects the whole structural health of the bridge system. Several of structural defects of bridges are due to the bridge deck geometry and deck condition. Thus, it is essential to build bridge deck systems that have long-term durability and require less maintenance (Kim and Jeong 2006, Brown

---

\*Corresponding author, Assistant Professor, E-mail: [dehestani@gmail.com](mailto:dehestani@gmail.com)

<sup>a</sup>MSc. Graduate Student, E-mail: [alizade.nit@gmail.com](mailto:alizade.nit@gmail.com)

and Berman 2010). In the early 1980's, Exodermic bridge deck that consist of steel profiles and concrete was developed by Neal Bettigole (Versace and Ramirez 2004), a consulting bridge engineer in New Jersey. Allahyari *et al.* (2014) experimentally evaluated the static and dynamic properties of the Exodermic bridge deck with alternative perfobond shear connectors. The weight of the deck is about 40% of common reinforced concrete slab. The experimental result showed that the first mode is the most effective mode among others. Also, the first four modes are the rigid translational motion modes, and the next two modes seem to be rigid rotational motion modes around a horizontal axis. In addition, Failure of the deck under positive bending was punching-shear.

The ultimate behavior of a steel-concrete composite deck with profiled steel plate and perfobond rib shear connectors was experimentally investigated by Kim and Jeong (2010). Typically, the weight and thickness of the steel-concrete deck is less than conventional reinforced concrete decks, so they can be implemented in a longer span, but their resistance against corrosion is low and they have high maintenance costs. Fiber reinforced polymers (FRP) composites have introduced a promising solution to solve prevalent problems in steel-concrete decks. The FRP composites have superior material properties such as high specific stiffness, specific strength, corrosion resistance, light weight, and durability. In recent years, the interest in using FRP in construction field has significantly increased worldwide (2009).

Gan *et al.* (1999) evaluated several cellular deck panels with different cross-sectional profiles based on finite element analysis. The specimens consist of hexagonal (H), triangle (T) and rectangular. Their numerical assessment covers the global and local stiffness, the maximum stresses, and buckling strength. The panels with 3-cell rectangular section can provide better properties in local stiffness and buckling strength than the T and H section panels.

Reising *et al.* (2004) tested four different fiber-reinforced polymer decks. They examines whether four composite deck are able to realize many of the expected benefits of using FRP composites instead of conventional reinforced concrete bridge decks. Installation matter, connection details, and specific construction techniques for each deck are explained. The results show that FRP deck systems could significantly reduce the installation time, and avoid lane closures in comparison to standard reinforced concrete decks.

Zi *et al.* (2008) experimentally investigated the behavior of an orthotropic bridge deck made of GFRP and polyurethane foam. The bridge deck composed of GFRP cells with rectangular holes filled with foam to improve the structural behavior in the transverse direction. Result shows that, when the GFRP bridge deck was filled with foam, the structural behaviors in the transverse direction such as the nominal strength and stiffness were greatly improved. Because of the low density of the foam, the bridge deck was still light enough while the structural properties were improved significantly.

Brown and Berman (2010) investigated the behavior of two glass fiber-reinforced polymer bridge decks and concluded that GFRP decks are a good alternative to the old steel arched deck.

In spite of all these advantages of FRP decks that mentioned, FRP composites are still too expensive to compete with conventional materials that used in civil engineering. Therefore, combinations of FRP and conventional materials have recently been studied by a number of researchers to make the best use of materials. The advantages of composite decks include the cost effectiveness and the ability to optimize the cross section based on material properties of each part.

Hillman and Murray (1990) proposed the innovative idea of a hybrid FRP-concrete decks. They suggested the combination of pultruded FRP sections and concrete to form lightweight deck. The

FRP section was used as reinforcement and a permanent formwork. Most of the concrete was located above the neutral axis of the hybrid deck. By these methods, the weight of composite decks reduced more than 50% compared with conventional concrete decks.

Bakeri and Sunder (1990) conducted numerical studies on composite bridge deck that made of a simply curved membrane of FRP composites filled with concrete. They concluded that the composite deck was desirable, especially from the view point of cost.

An experimental and analytical study was performed on composite FRP- concrete beams by Saiidi *et al.* (1994). An epoxy resin was used for bonding CFRP elements and a concrete slab in their model. They concluded that mechanical connectors are needed to develop composite action of the deck in addition to epoxy resin.

Deskovic *et al.* (1995) proposed a composite beam consisted of GFRP box section, a layer of concrete in compression zone and a CFRP laminate in tension zone. Web-fracture, bond failure, and web-buckling were examined. Their study demonstrated the feasibility and cost-effectiveness of composite beam.

Kitane *et al.* (2004) examined flexural performance of hybrid FRP-concrete beams. In their design, three trapezoidal boxes of FRP laminates were assembled with a layer of concrete in the compression zone of sections. Their new design reduced the initial costs and increases the stiffness of GFRP composite decks. The results show trapezoidal box sections with an inclination angle impart reduced shear stresses at the interface of next box sections.

By using this information, Alnahhalet *et al.* (2008) developed a HFRPC bridge deck consisting of trapezoidal GFRP cell units covered by an outer GFRP shell. A thin layer of concrete is located between the inner GFRP trapezoidal cell and the outer GFRP trapezoidal cell to increase the stiffness of the deck and to reduce local deformations due to point loads. The composite action between the hybrid deck and steel girders is experimentally and numerically investigated. In addition, the effective flange width in the composite deck acting compositely with the steel girders is evaluated at service conditions. The experimental and finite element results showed that the structural performance of the FRP-concrete deck is higher than AASHTO specifications. Moreover, it was observed that the hybrid deck and the steel girders are interacting in a partially composite action under service load. Effective width calculations of the hybrid deck showed that the effective flange width for composite decks is less than AASHTO prescribed effective width for concrete decks.

The performance of hybrid FRP-concrete trapezoidal bridge deck under sustained and fatigue loading was experimentally investigated by Warn and Aref (2010). The experimental results demonstrated that the deck could be a practical alternative to traditional reinforced concrete decks. The proposed HFRPC bridge deck and shear stud connection detail sufficiently resisted fatigue induced reduction. Furthermore, the partial composite action between the steel girders and the deck was not altered after the 2 million cycles.

Keller *et al.* (2007) tested composite beams consisting of FRP plate with T-up stands in tensile, lightweight concrete as a core (LC), and thin layer of ultra high strength fiber reinforced concrete for the compression zone. Experimental evaluation was conducted on several hybrid beams with two types of low and high density concrete core and two types of interface between FRP and concrete core; unbounded, (only mechanical shear connection) and bonded with an epoxy adhesive. The ultimate loads of the beams increased due to bonding. However, the failure mode of the beam changed from ductile to brittle. The ultimate load of the beams that used a LC with a higher density, increased. The manufacturing of the beams proved to be economic in that epoxy and concrete layers were rapidly and easily applied wet-in-wet without intermediate curing times.

Sutter *et al.* (2014) conducted experimental and analytical studies on composite beams consisting of U-shape section and hollow core elements that made of fire safe HPTRCC material. They used ultra-high performance concrete and CFRP at upper and lower side of the hollow element, respectively. They concluded that a composite beam, with the same stiffness as the traditional reinforced concrete beams, has greater bearing capacity, despite of being lighter.

Idris and Ozbakkaloglu (2014) examined flexural performance of hybrid beams. In their design, the inner steel tube placed inside the outer FRP tube and the space between them filled with concrete. Test results showed that the diameter and thickness of the inner steel tube significantly influenced the flexural behavior of beam and increasing the concrete strength increases the flexural capacity of beam without influencing their ductility.

### *1.1 Research significance*

As stated above, in most cases, experimental studies were performed to evaluate the behavior of composite girders. Due to the high cost of experimental studies and their long duration, it is common to propose the finite element method to study the behavior of this type of structures to allow more purposeful estimates by reducing the cost of testing. The main purpose of the present study is numerical modeling of the composite girders with finite element analysis and comparing the results of numerical models with existing experimental results. By analyzing the important parameters, a good insight and prediction of the composite behavior can be achieved. The influences regarding the alteration of various parameters on composite girder would provide a proper and convenient approach for design procedure.

## **2. Numerical modeling**

In order to evaluate the behavior of composite girders by finite element method, at first, numerical model of composite girder that has been experimentally investigated by Fam and Honickman (2010) was generated. The finite element (FE) analysis results were validated by all respective experimental results and then parametric studies were performed.

### *2.1 Summary of experimental program*

Fam and Honickman (2010) conducted experimental and analytical studies on new composite girders. As shown in Fig. 1(a) the girder consisted of a hat-shape GFRP trapezoidal section (254 mm deep×610 mm wide×3350 mm long) and a GFRP plate (9.5 mm thick). Fig. 1(b) and (c) shows the cross-section of G1 (with a 60 mm concrete slab that optimally designed to be completely in compression) and G2 (without a concrete slab). In specimen G1 the concrete slab connected to the top GFRP plate with both epoxy adhesives and steel shear connectors and in specimens G1 and G2, Adhesive and mechanical bond systems were employed to connect the top GFRP plate to the flanges of the GFRP trapezoidal hat-shape section. The material properties of the GFRP composites are shown in Table 1. The concrete compression strength was 52 MPa when the girders were tested. The end diaphragms of girders filled with cementitious grout with a compressive strength of 36 MPa. The girders were tested in four-point bending with a span of 3100 mm, and a 400 mm distance between the two loads (Fig. 2). The load was monotonically applied at a loading rate of 1 mm/min. The strain gauges were installed at the mid-span of the

girder, on the top of concrete slab and bottom of the hat-shape section. Summary of experimental specimens are shown in Table 2. The test results included load carrying capacity and failure modes, as summarized in Table 3.

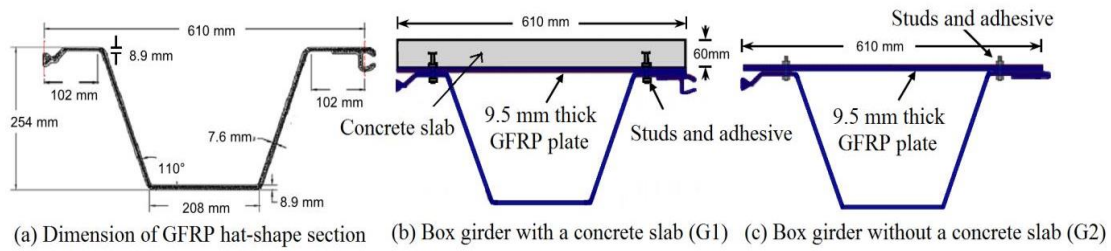


Fig. 1 Configurations of experimental specimens (unit: mm)

Table 1 Material properties of GFRP composites

		Hat -Shape section		GFRP plate	
		Longitudinal	Transverse	Longitudinal	Transverse
Tensile modulus (GPa)	Tension	26.2	11	12.4	6.9
	Compression	26.2	11	12.4	6.9
Tensile strength (MPa)	Tension	517	138	137.5	68.7
	Compression	345	172	165	110

Table 2 Summary of experimental specimens

Girder	Cross-section	Bond mechanism	Test configuration	Bending orientation
G <sub>1</sub>	Box-girder with a concrete slab (Fig. 1(b))	Shear studs and adhesive bond	4-point bending Span = 3100 mm Loads spaced at 400 mm	Positive
G <sub>2</sub>	Box-girder without concrete slab (Fig. 1(c))			

Table 3 Details of girder specimens

Specimen	Concrete deck	Failure load (kN)	Failure mode
Girder G <sub>1</sub> - E <sup>a</sup>	Yes	430	Concrete crushing
Girder G <sub>1</sub> - F <sup>b</sup>	Yes	425	Concrete crushing
Girder G <sub>2</sub> - E <sup>a</sup>	None	230	GFRP crushing
Girder G <sub>2</sub> - F <sup>b</sup>	None	240	GFRP crushing

<sup>a</sup>Experimental

<sup>b</sup>FE prediction

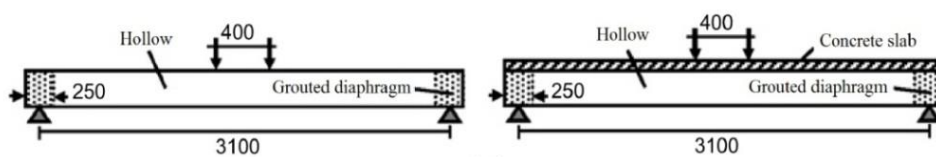


Fig. 2 Loading scheme

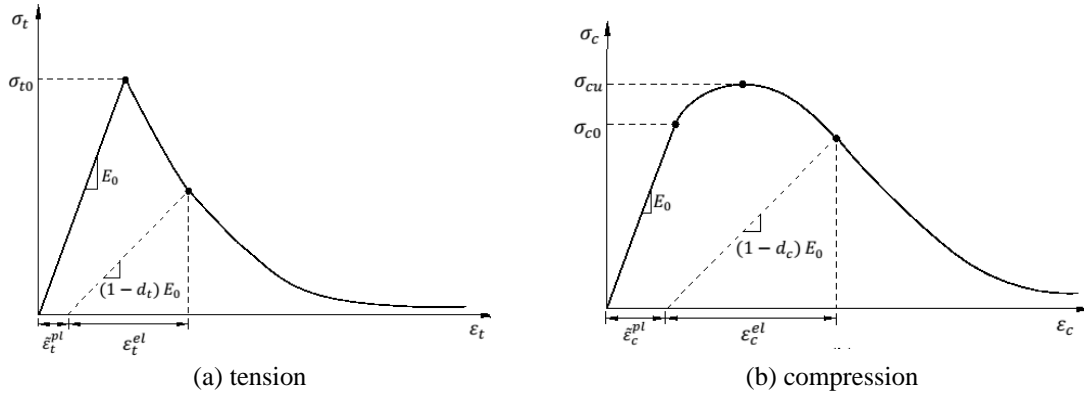


Fig. 3 Response of concrete to uniaxial loading

## 2.2 Implementation of finite element analysis in ABAQUS

A three-dimensional finite element analysis was carried out to evaluate the flexural behavior of the GFRP-concrete girder using ABAQUS (2004). It was decided to model the specimens G1 (with a concrete slab) and G2 (without a concrete slab) in this study. The following summarizes the numerical approach.

### 2.2.1 Constitutive modeling and elements

The concrete damaged plasticity model was adopted to model the concrete slab. This model is based on the assumption of isotropic damage and is designed for applications in which the concrete is subjected to arbitrary loading conditions, containing cyclic loading. The model considers the reduction of the elastic stiffness caused by plastic straining both in tension and compression. It supposes that the main two failures are tensile cracking and compressive crushing of the concrete material. The progression of the yield (or failure) surface is controlled by two hardening variables,  $\tilde{\epsilon}_t^{pl}$  and  $\tilde{\epsilon}_c^{pl}$ , linked to failure mechanisms under tension and compression loading, respectively.  $\tilde{\epsilon}_t^{pl}$  and  $\tilde{\epsilon}_c^{pl}$  are tensile and compressive equivalent plastic strains, respectively. The model assumes that the uniaxial tensile and compressive response of concrete is characterized by damaged plasticity, as shown in Fig. 3. Under uniaxial tension the stress-strain response follows a linear elastic relationship until the value of the failure stress is reached to  $\sigma_{t0}$ . The failure stress corresponds to the beginning of micro-cracking in the concrete material. Beyond the failure stress the formation of micro-cracks is represented macroscopically with a softening stress-strain response, which causes strain localization in the concrete structure. Under uniaxial compression the response is linear until the value of initial yield,  $\sigma_{c0}$ . In the plastic regime the response is typically characterized by stress hardening followed by strain softening beyond the ultimate stress,  $\sigma_{cu}$ .

In order to simulate the responses of two control girder specimens  $G_1$  and  $G_2$ , all material parameters were initially calibrated. The values adopted for the relevant material parameters, namely the angle of dilation, the eccentricity, the ratio of equibiaxial to uniaxial compressive stress  $f_{b0}/f_{c0}$ , the ratio of the second stress invariant on the tensile meridian to that on the compressive meridian at initial yield  $K_c$  and the viscosity parameter were 54, 0.1, 1.16, 0.667 and 0 respectively. The stress-strain response of concrete in compression was defined according to

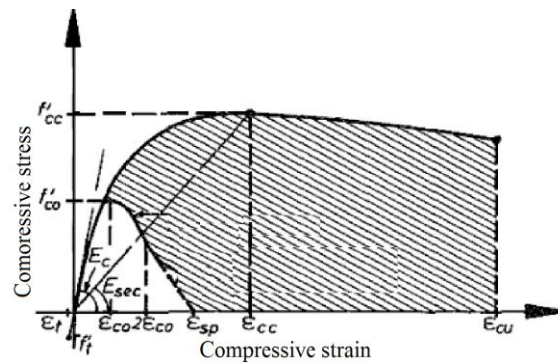


Fig. 4 Mander stress- strain model for monotonic loading of confined and unconfined concrete

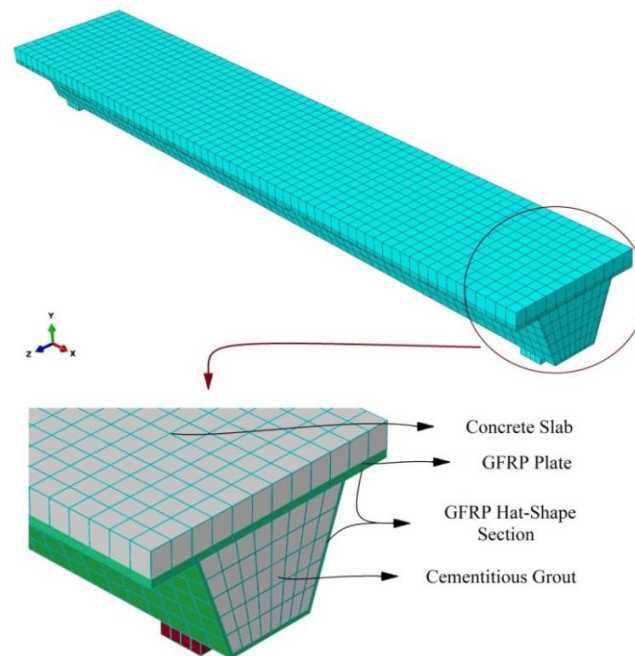


Fig. 5 Finite element mesh of composite girder

Mander *et al.* (1988) as shown in Fig. 4. The tension stiffening Response was defined in terms of tensile stress and axial deformation according to Reinhardt *et al.* (1986). The Young's modulus and tensile strength were considered according to ACI (1999). The FRP is also modeled as orthotropic material. The concrete and FRP was modeled by 8-node linear brick elements (C3D8).

### 2.2.2 Geometry and boundary conditions

The Finite element model of composite girder is shown in Fig. 5. In order to make computational time minimum and achieving the highest accuracy simultaneously based on comprehensive mesh convergence studies, mesh size adopted with a maximum element size of 50 mm (1.5% of the specimen length). Boundary conditions were applied to simulate a simply-supported condition by constraining necessary nodes in translation at supports of the specimens.

Nonlinear iterations were solved by using Newton-Raphson method.

### 3. Validation of analytical model

The structural behavior of hat-shape composite girders (with and without concrete slab) has been studied through the finite element method (FEM), and the results of numerical analysis compared with experimental results of other researchers.

#### 3.1 Hat-shape composite girder with a concrete slab

Table 3 summarizes the ultimate loads of girders. The specimen with concrete slab (Girder G<sub>1</sub>-E) failed at a load of 430 kN, while the predicted failure load was 1.1% lower (425 kN for Girder G<sub>1</sub>-F). Fig. 6 shows the load-displacement responses at mid-span of composite girder with a concrete slab in both experimental and numerical cases which conform to each other quite well in ultimate strength and stiffness. The Numerical results demonstrate that the neutral axis of this specimen is located about 55-60 mm from the top which almost remains constant until the failure occurs. It shows that concrete slab is totally under a compression which is so desirable. The failure of experimental specimen is caused by concrete crushing at mid-span of composite girder (2010). In addition, Fig. 7 shows the plastic strain and concrete failure in the numerical specimen. The different components of plastic strain and the principal plastic strain are the best criteria for studying tension (cracking) and compression (crushing) failure in numerical modeling of concrete. According to Fig. 7, the maximum amount of plastic strain which exists in the middle zone of the girder is 3.5% that is rather high and shows the concrete crushing and extensive damage. Generally, the failure of numerical specimen is similar to experimental one that is due to concrete crushing. Von Misses equivalent stress in concrete slab is also shown in Fig. 8, which indicates that the largest amount of stress is on the middle zone of girder. As it has been stated before,

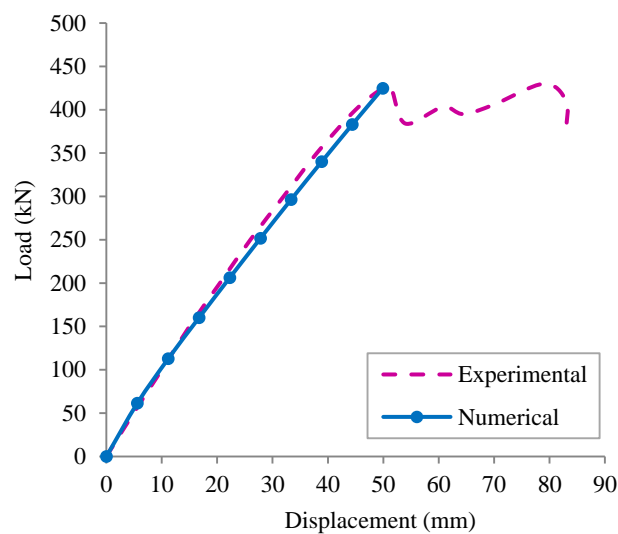


Fig. 6 Load-displacement response at mid-span of specimens (G<sub>1</sub>)

Printed using Abaqus/CAE

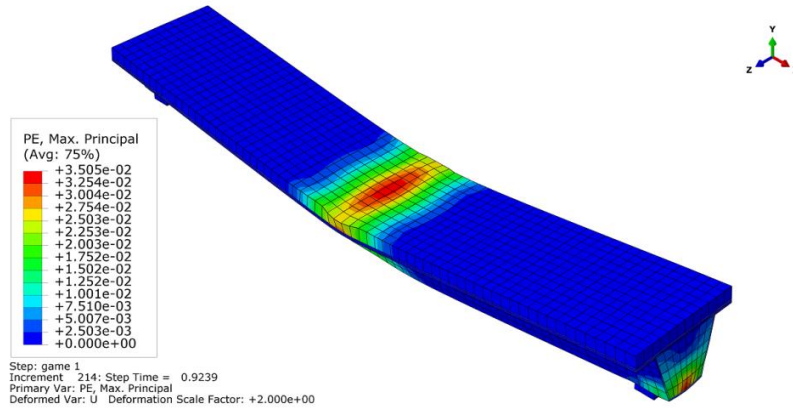


Fig. 7 Principal plastic strain and failure mode of numerical specimen ( $G_1$ )

Printed using Abaqus/CAE

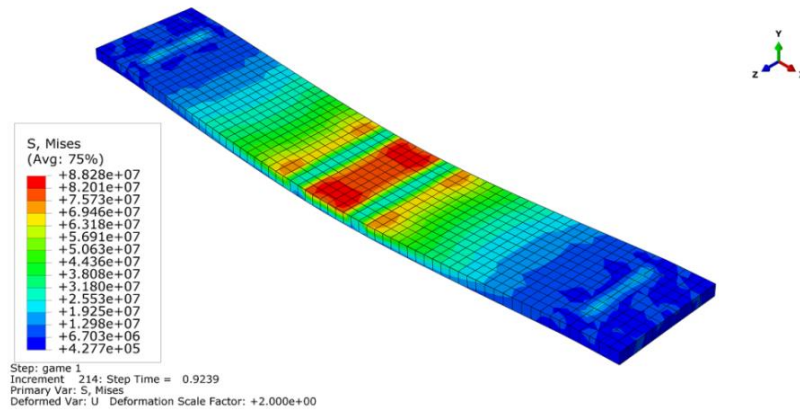


Fig. 8 Von Mises equivalent stress in concrete slab ( $G_1$ )

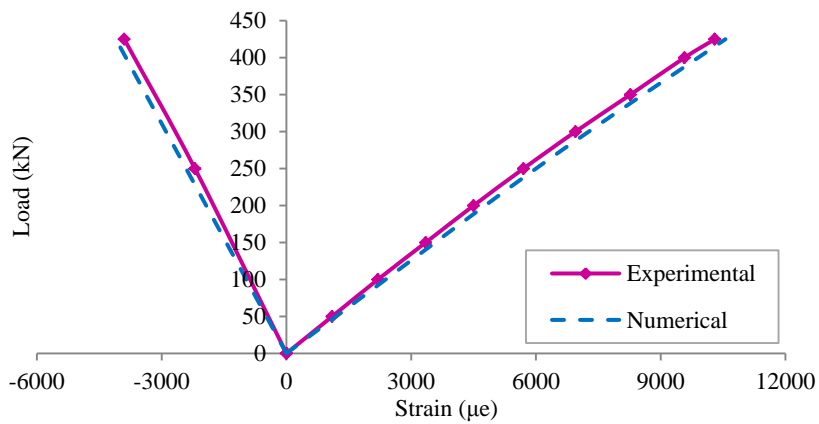


Fig. 9 Load-strain response at mid-span of specimens ( $G_1$ )

different strain gauges were installed in the upper and lower surfaces of the girder (on the concrete and under the hat-shape section). The values of strain in numerical specimen were measured for the same points of experimental one, and the resultant of load-strain responses for both the experimental and numerical specimens are shown in Fig. 9. It reveals that numerical results shows very good agreement with the experimental ones.

### 3.2 Hat-shape composite girder without a concrete slab

As shown in Table 3, the experimental specimen without a concrete slab (Girder G<sub>2</sub>-E) showed a decrease of 46.5% in the ultimate load when compared to experimental Girder G<sub>1</sub>-E with the concrete slab, and the corresponding prediction exhibited an increase of 4.3% (Girder G<sub>2</sub>-F).

Fig. 10 shows the load-displacement responses at mid-span of the composite girder without a concrete slab. The diagrams in both experimental and numerical cases conform to each other quite well in terms of ultimate strength and stiffness. As investigated, the neutral axis of this specimen is located about 115-120 mm from the top GFRP plate and almost remains fixed until the failure load. The failure of experimental specimen of the girder without a concrete slab is caused by local buckling and GFRP plate crushing (2010). The principal stress of GFRP plate in the numerical model is 173 MPa at mid- span of the girder (Fig .11) and the ultimate compression strength of the GFRP plate in experimental specimen is 165 MPa (Table 1), so it can be concluded that failure occurred in GFRP plate in that point of numerical specimen. Generally, the failure of the numerical specimen like the experimental one is due to crushing and buckling of the GFRP plate.

According to the diagrams and figures above, experimental and numerical results conform to each other quite well in terms of ultimate strength, stiffness, damage, and the behavior as result. Hence, the results of the numerical analyses done through FEM in this research are reliable, and it could be said that the behavior of hat-shape composite girders can be studied through numerical methods, without conducting any costly experiment.

## 4. Parametrical study

After ensuring the verification of the numerical modeling through FEM, the parametric study of the hat-shape composite girder were done with a change in compression strength of the concrete slab, the elasticity modulus of the hat-shape section, and GFRP plate, altering the material of the GFRP hat-shape section to steel and aluminum, and finally changing the section of the composite girder to a concrete-filled one. The hat-shape composite girder with a concrete slab (G1) was chosen as the numerical control specimen. In all analyses, the type of elements and modeling was the same as those in the verification part.

### 4.1 Effect of concrete strength

The compression strength ( $f_c'$ ) of the experimental specimens was 52.2 MPa. As shown in Fig. 12, the concrete strength was changed to 30, 40, 60 and 70 to evaluate its effects on the behavior of the composite girder. By about 34% increase in compression strength of the concrete slab (52.2 MPa to 70 MPa) the load capacity of the girder increased about 16%, whilst, by 42% decrease in  $f_c'$  the load capacity decreased about 36%. The failure of specimens was due to the concrete crushing in the compression area again.

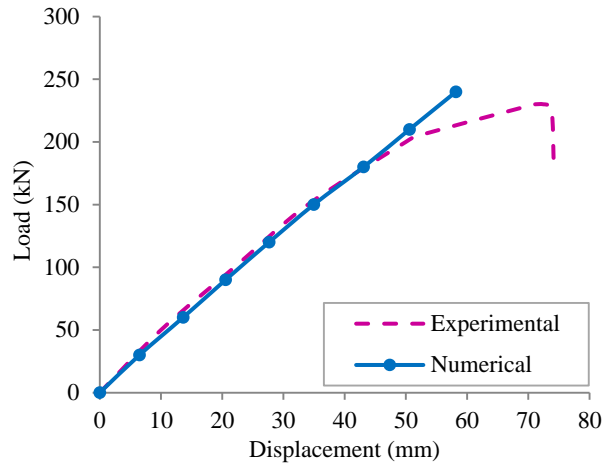


Fig. 10 Load-displacement response at mid-span of specimens ( $G_2$ )

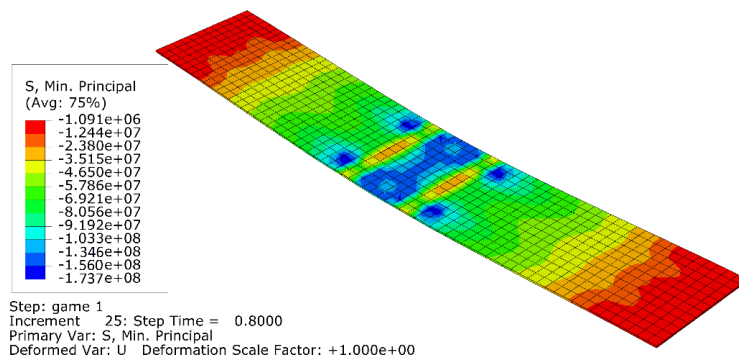


Fig. 11 Principal stress of GFRP plate and failure mode of numerical specimen ( $G_2$ )

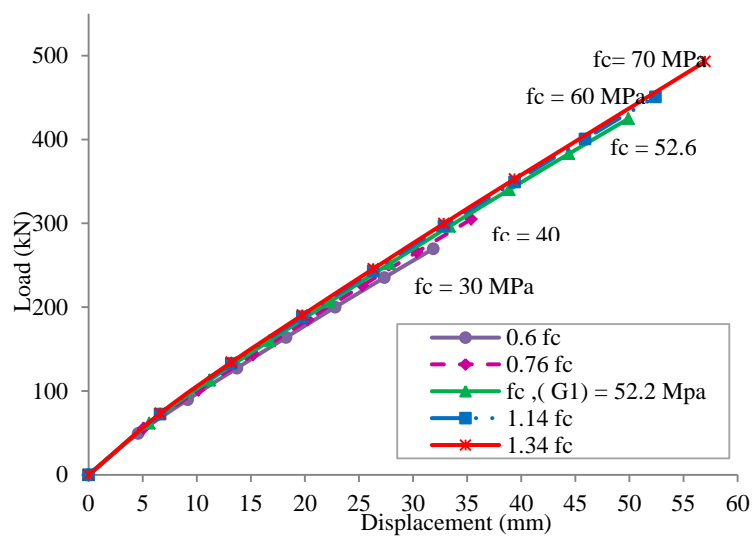


Fig. 12 Effect of concrete strength on load- displacement diagram

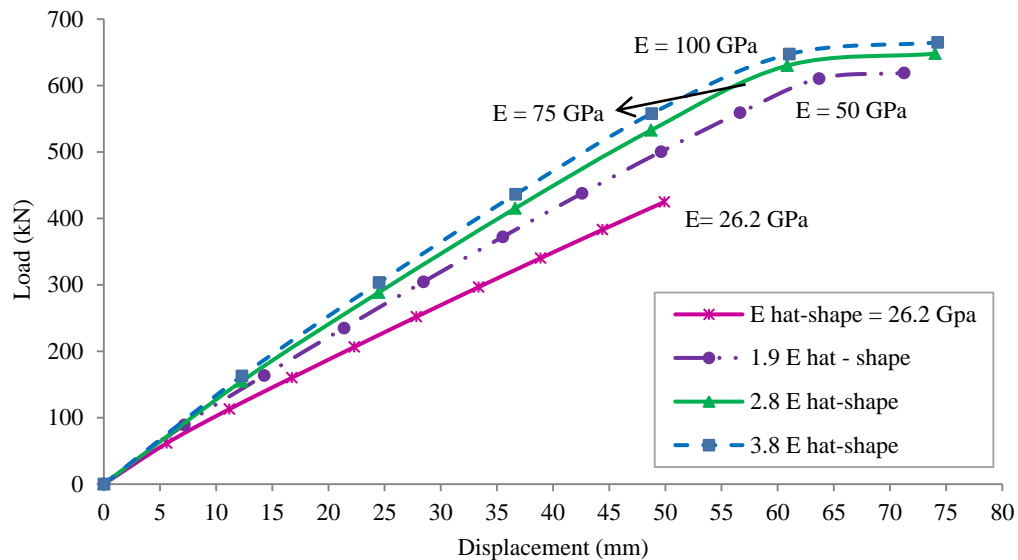


Fig. 13 Effect of elasticity modulus of hat-shape section on load–displacement diagram

#### 4.2 Effect of elasticity modulus of hat-shape section

The elasticity modulus of hat-shape section in the numerical control specimen was 26.2 GPa. As shown in Fig. 13, the value of the elasticity modulus of hat-shape section was changed to 50, 75 and 100, which are all commercially available, to examine its effect on the behavior of the composite girder. By changing the elasticity modulus from 26.2 GPa to 100 GPa, the load capacity of the girder increases about 56%. The load capacity increment could be the result of raising the stiffness of the specimens which is caused by the increase in the elasticity modulus of the hat-shape section.

#### 4.3 Effect of elasticity modulus of GFRP plate

Fig. 14 shows another parametric study to evaluate the effect of elasticity modulus of GFRP plate influencing the behavior of the GFRP girders. Increasing elasticity modulus has an insignificant effect on stiffness. It, however, increases the load capacity by about 33% for a specimen that its elasticity modulus changed from 20 GPa to 100 GPa.

#### 4.4 Effect of altering the material of GFRP plate and hat-shape section to steel

In order to examine the efficacy of the GFRP box girders, a parametric study was conducted to compare the GFRP box girder with steel ones. In order to do so, at first, the GFRP plate was changed to steel (specimen B<sub>1</sub>), then, the GFRP hat-shape section was changed to steel (specimen B<sub>2</sub>), and finally, the GFRP plate with a hat-shape section was changed to steel (specimen B<sub>3</sub>). In this section, all thicknesses are the same as control specimen G<sub>1</sub>, that shown in Fig. 1. Table 4 provides the Constitutive material of specimens in parametric study. Mechanical properties of steel material are shown in Table 5. The load-displacement responses of the different cases of the

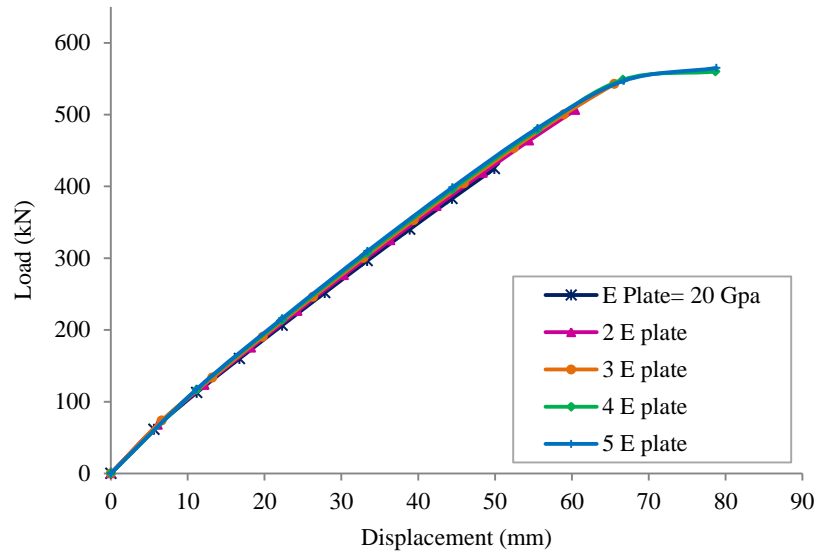


Fig. 14 Effect of elasticity modulus of GFRP plate on load-displacement diagram

Table 4 The constitutive material of girders in parametric study

Girder	Constitutive material	
	Hat-Shape section	plate
G <sub>1</sub>	GFRP	GFRP
B <sub>1</sub>	GFRP	Steel
B <sub>2</sub>	steel	GFRP
B <sub>3</sub>	Steel	Steel
B <sub>4</sub>	GFRP	Aluminum
B <sub>5</sub>	Aluminum	GFRP
B <sub>6</sub>	Aluminum	Aluminum

changing the material from GFRP to steel are shown in Fig. 15. The results indicate that replacing the GFRP plate by a steel one (specimen B<sub>1</sub>), which was close to the neutral axis, had no significant effect on the stiffness of the composite girder but increased the load capacity of the girder by 38%. Also the stiffness of the hat-shape composite girder with a concrete slab (specimen G<sub>1</sub>) and its load capacity increased 66% by changing the hat-shape section and the plate on it from GFRP to steel (specimen B<sub>3</sub>). However, since the specimen G<sub>1</sub> was 364 kg and the specimen B<sub>3</sub> was 644 kg, it can be said that the strength-to-weight ratio decrease by about 6% with a change in the material of the girder from GFRP to steel. As illustrated in Fig. 15, the specimen B<sub>1</sub> and its load-displacement responses are almost linear up to ultimate load due to the low volume of the steel in this specimen and the proximity of the plate to the neutral axis, so other constitutive materials (GFRP and concrete) dominated the behavior of the girder. The stiffness increment in specimen B<sub>2</sub> and B<sub>3</sub> was significant and yielding of the steel created the desired ductility in these two specimens.

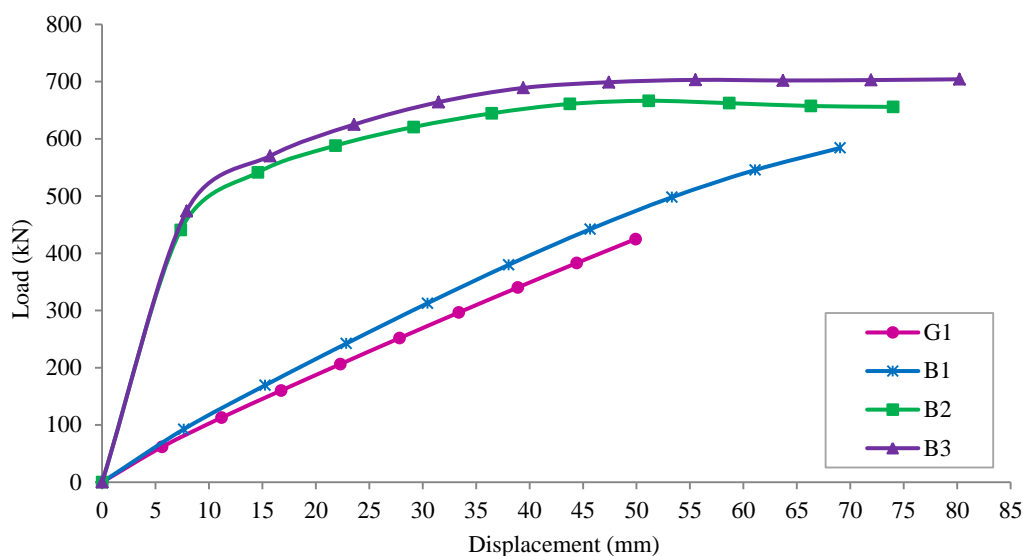


Fig. 15 Load-displacement responses of the different cases of the material change from GFRP to steel

Table 5 Mechanical properties of steel and Aluminum

Material	Modulus (GPa)	Strength (MPa)		Poisson's ratio
		Yield	Ultimate	
Carbon steel A36	206	250	475	0.3
Aluminum 6061-T6	70	276	310	0.33

#### 4.5 Effect of altering the material of GFRP plate and hat-shape section to aluminum

In this part, the material of the GFRP section was changed to aluminum 6082-T6 (Table 5) to examine the effect of the constitutive material on the behavior of composite girder. For this purpose, at first, the GFRP plate was changed to aluminum specimen B<sub>4</sub>. Then, the hat-shape section which was made of GFRP was changed to aluminum (specimen B<sub>5</sub>), and finally the GFRP plate with a hat-shape section was changed to aluminum section (B<sub>6</sub>). The thickness of sections in all aluminum specimens are the same as control specimen G<sub>1</sub>, that shown in Fig. 1. The load-displacement responses of the different cases of the material changing are shown in Fig. 16. Changing the material of the GFRP plate to aluminum had an insignificant effect on stiffness of the composite girder but increased the load capacity of the girder by about 32%. By changing the material of the hat-shape section and the GFRP plate from GFRP to aluminum, the stiffness of composite girder increased considerably, and its ultimate load capacity increased by about 70%. However, since the specimen G<sub>1</sub> was 364 kg and the specimen B<sub>6</sub> was 414 kg, it can be said that the ratio of strength-to-weight increase by about 51% with a material changing from GFRP to aluminum. The failure of the specimens occurred due to the aluminum yielding and its plastic deformations and crushing of the concrete slab.

Finally, for a better interpretation, the diagrams of changing the material from GFRP to steel and aluminum were compared in Fig. 17. The stiffness of the aluminum used in this study was not

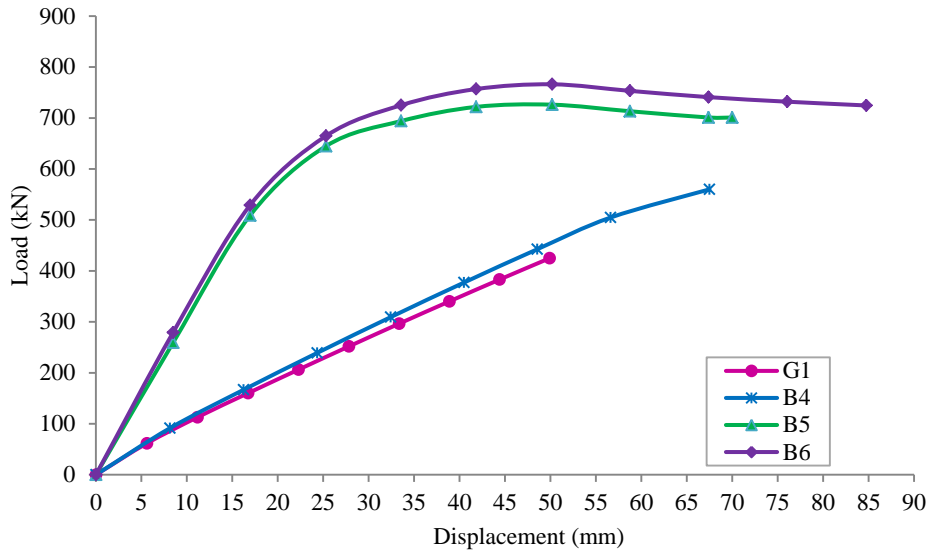


Fig. 16 Load-displacement responses of the different cases of the material change from GFRP to aluminum

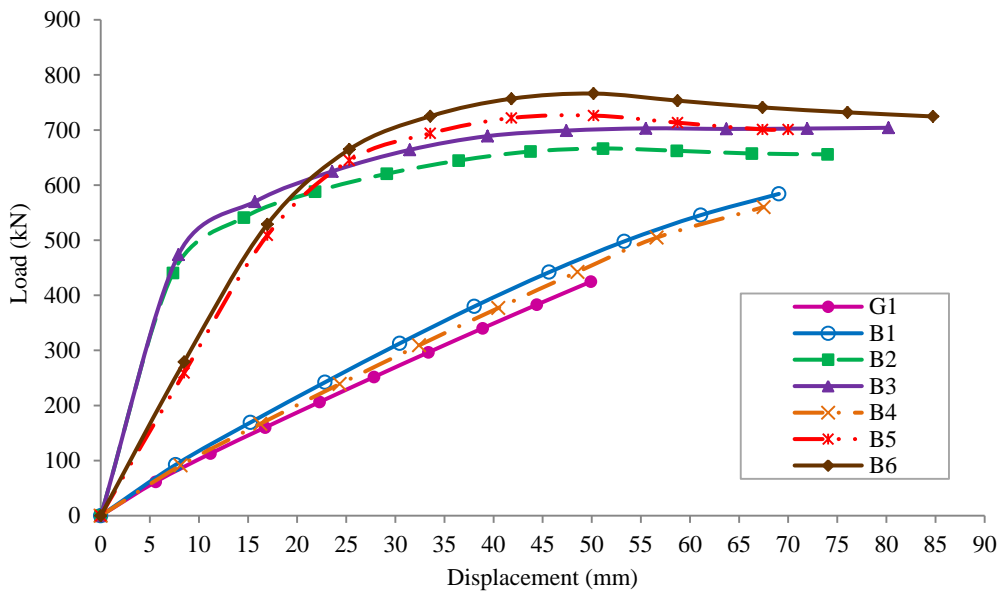


Fig. 17 Load-displacement responses of the different cases of the material change from GFRP to steel and aluminum

as stiff as steel, but it had a higher yield point, which clearly can be seen in Fig. 17. The aluminum specimens were not as stiff as the steel ones, but reach the yield point at a higher load.

#### 4.6 Effect of cross-sectional configuration

In first step of this part, the GFRP plate of the numerical control girder was removed and the

whole section was filled with concrete with compression strength of 52.2 MPa (specimen B<sub>7</sub>). The behavior of this girder was numerically investigated. Then, a rectangular hole with dimensions of 0.245×0.15 m was created in the cross section and the performance of this hollowed concrete core specimen (B<sub>8</sub>) was studied (Fig. 18). Details of specimens are shown in Table 6. The load-displacement of the totally concrete-filled girder and the hollowed concrete core specimen are shown in Fig. 19.

Generally, the ultimate load capacity increases with above-mentioned change in the cross-sectional configuration of the specimen G<sub>1</sub>, but the ratio of load capacity to weight decreases, because of notable increase in the weight of the specimens. The hollowed concrete core in the tension region (specimen B<sub>8</sub>), reduced the stiffness and the ultimate load capacity by about 12% in comparison with the specimen that totally filled with concrete. Overall, the voided system has a 24% higher strength-to-weight ratio than the totally filled section.

Table 6 Detail of specimens

Girder	Cross- section configuration
G <sub>1</sub>	Hat-Shape section with concrete slab
B <sub>7</sub>	Totally filled with concrete
B <sub>8</sub>	Hollowed concrete core

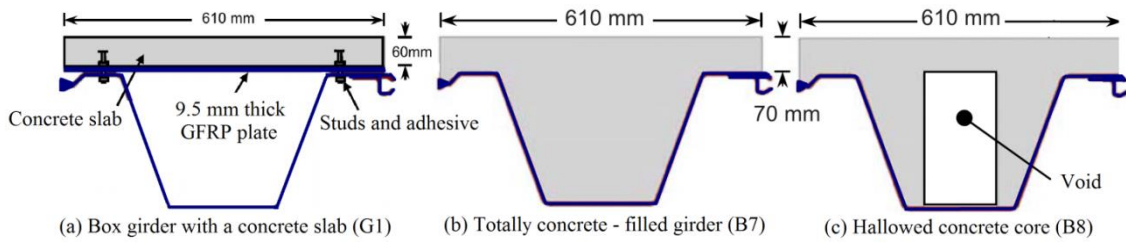


Fig. 18 Cross-sectional configuration of specimens G<sub>1</sub>, B<sub>7</sub>, B<sub>8</sub>

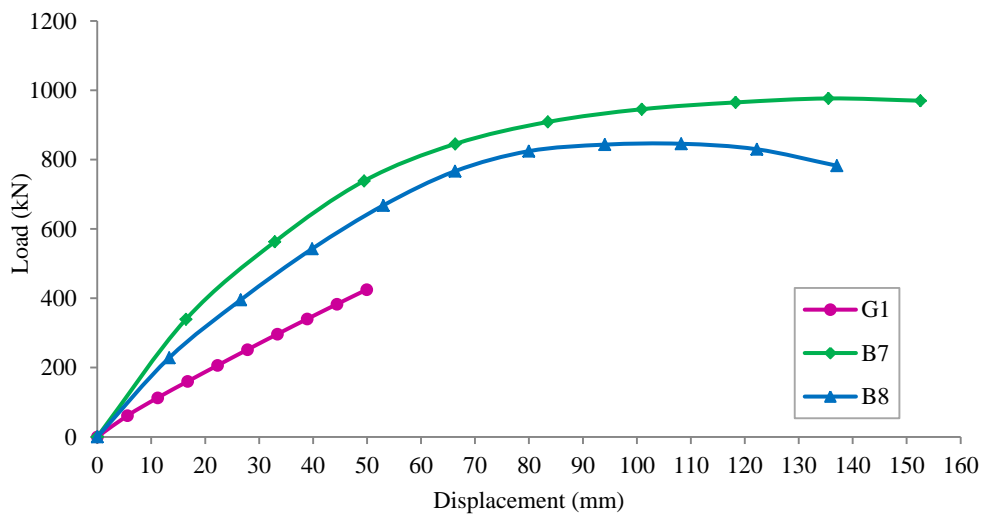


Fig. 19 Load-displacement responses of totally concrete-filled and the hollowed concrete core specimens

## 5. Conclusions

This research has presented a numerical investigation for the flexural behavior of built-up hat-shape GFRP box girders with and without concrete slab. A three-dimensional modeling approach was developed and validated using experimental data. Emphasis was on the ultimate strength, failure modes, deformability, and strength-to-weight ratio. The following results were achieved.

- The FE model predicted the flexural behavior and failure modes of GFRP box girders with and without concrete slabs with an excellent accuracy when compared with experimental results.
- Increasing the concrete strength has a negligible effect on the stiffness; it, however, increases ultimate load capacity of the hat-shape composite girder as predicted.
- Increasing the elasticity modulus of the hat-shape section and GFRP plate increases ultimate load capacity and stiffness of the composite girder.
- Changing the material of the hat-shape section and the GFRP plate from GFRP to steel increases the stiffness and ultimate load capacity of the section to a great extent, but it decreases the strength-to-weight ratio. Also since the steel has a considerable plastic deformations (so it doesn't fail in a brittle manner unlike the GFRP), the ductility of the girder increases in comparison with the numerical control specimen.
- Changing the material of the hat-shape section and the plate on that from GFRP to aluminum increases the stiffness of the composite girder, load capacity, ductility, and the strength-to-weight ratio. A comparison between the steel and aluminum specimens indicates that the aluminum specimens are less stiff and yield at a higher load.
- Changing the Cross-Sectional Configuration of the composite girder to the concrete-filled specimen increases both the stiffness and load capacity. Posing a hole in the section of the concrete-filled specimen reduces the load capacity in comparison with the concrete-filled specimen; however, the strength-to-weight ratio goes up conversely.

## Acknowledgments

This research is supported by the Housing and Urban Development Research Center via grant No. 18672 and Mazandaran Road and Urban Department of Iran. The research job has been carried out in Babol Noshirvani University of Technology in Iran.

## References

- ACI Committee 318 (1999), Building code requirements for structural concrete: (ACI 318-99) and commentary (ACI 318R-99), Farmington Hills, Mich, American Concrete Institute.
- Allahyari, H., Dehestani, M., Beygi, M.H., Neya, B.N. and Rahmani, E. (2014), "Mechanical behavior of steel-concrete composite decks with perfobond shear connectors", *Steel Compos. Struct.*, (17), 339-358.
- Alnahhal, W., Aref, A. and Alampalli, S. (2008), "Composite behavior of hybrid FRP-concrete bridge decks on steel girders", *Compos. Struct.*, 84(1), 29-43.
- Bakeri, P.A. and Sunder, S.S. (1990), "Concepts for hybrid FRP bridge deck systems", *Serviceab. Durab. Constr. Mater.*, ASCE, 1006-1015.
- Brown, D.L. and Berman, J.W. (2010), "Fatigue and strength evaluation of two glass fiber-reinforced polymer bridge decks", *J. Bridge Eng.*, 15(3), 290-301.
- Deskovic, N., Triantafillou, T.C. and Meier, U. (1995), "Innovative design of FRP combined with concrete:

- short-term behavior”, *J. Struct. Eng.*, **121**(7), 1069-1078.
- De Sutter, S., Remy, O., Tysmans, T. and Wastiels, J. (2014), “Development and experimental validation of a lightweight Stay-in-Place composite formwork for concrete beams”, *Construct. Build. Mater.*, **63**, 33-39.
- Fam, A. and Honickman, H. (2010), “Built-up hybrid composite box girders fabricated and tested in flexure”, *Eng. Struct.*, **32**(4), 1028-1037.
- Gan, L.H., Ye, L. and Mai, Y.W. (1999), “Design and evaluation of various section profiles for pultruded deck panels”, *Compos. Struct.*, **47**(1), 719-725.
- Hibbitt, D., Karlsson, B. and Sorensen, P. (2004), ABAQUS Analysis User’s Manual, Pawtucket, USA.
- Hillman, J.R. and Murray, T.M. (1990), “Innovative floor systems for steel framed buildings”, *Proceedings of the IABSE Symp. Mixed Struct. Including New Material, International Association for Bridge and Structural Engineering*, Brussels.
- Idris, Y. and Ozbakkaloglu, T. (2014), “Flexural behavior of FRP-HSC-steel composite beams”, *Thin Wall. Struct.*, **80**, 207-216.
- Ji, H.S., Son, B.J. and Ma, Z. (2009), “Evaluation of composite sandwich bridge decks with hybrid FRP-steel core”, *J. Bridge Eng.*, **14**(1), 36-44.
- Keller, T., Schaumann, E. and Vallée, T. (2007), “Flexural behavior of a hybrid FRP and lightweight concrete sandwich bridge deck”, *Compos. Part A: Appl. Sci. Manuf.*, **38**(3), 879-889.
- Kim, H.Y. and Jeong, Y.J. (2006), “Experimental investigation on behavior of steel–concrete composite bridge decks with perfobond ribs”, *J. Construct. Steel Res.*, **62**(5), 463-471.
- Kim, H.Y. and Jeong, Y.J. (2010), “Ultimate strength of a steel–concrete composite bridge deck slab with profiled sheeting”, *Eng. Struct.*, **32**(2), 534-546.
- Kitane, Y., Aref, A.J. and Lee, G.C. (2004), “Static and fatigue testing of hybrid fiber-reinforced polymer-concrete bridge superstructure”, *J. Compos. Construct.*, **8**(2), 182-190.
- Mander, J.B., Priestley, M.J. and Park, R. (1988), “Theoretical stress-strain model for confined concrete”, *J. Struct. Eng.*, **114**(8), 1804-1826.
- Reinhardt, H.W., Cornelissen, H.A. and Hordijk, D.A. (1986), “Tensile tests and failure analysis of concrete”, *J. Struct. Eng.*, **112**(11), 2462-2477.
- Reising, R.M., Shahrooz, B.M., Hunt, V.J., Neumann, A.R., Helmicki, A.J. and Hastak, M. (2004), “Close look at construction issues and performance of four fiber-reinforced polymer composite bridge decks”, *J. Compos. Construct.*, **8**(1), 33-42.
- Saiidi, M., Gordaninejad, F. and Wehbe, N. (1994), “Behavior of graphite/epoxy concrete composite beams”, *J. Struct. Eng.*, **120**(10), 2958-2976.
- Versace, J.D. and Ramirez, J.A. (2004), Implementation of Full-Width Bridge Deck Panels: A Synthesis Study, No. FHWA/IN/JTRP-2003/24.
- Warn, G.P. and Aref, A.J. (2010), “Sustained-load and fatigue performance of a hybrid FRP-concrete bridge deck system”, *J. Compos. Construct.*, **14**(6), 856-864.
- Zi, G., Kim, B.M., Hwang, Y.K. and Lee, Y.H. (2008), “An experimental study on static behavior of a GFRP bridge deck filled with a polyurethane foam”, *Compos. Struct.*, **82**(2), 257-268.